

COMPARISON OF STRUCTURAL AND ACOUSTICAL ACTIVE NOISE CONTROL PERFORMANCE OF THE FOKKER 100 BASED ON EXPERIMENTAL SIMULATION MODELS

H. Van der Auweraer *, T. Martens *, E. Waterman **,
T. Olbrechts ***, F. Augusztinovicz ***

* LMS International, Belgium

** Fokker Aircraft BV, The Netherlands

*** KU Leuven, Belgium

ABSTRACT

The present paper compares the performance of acoustical and structural secondary sources for active noise control in an aircraft cabin. In order to predict the performance of such systems and to optimise the actual configuration in terms of number and location of actuators and sensors, a methodology combining in-flight data with vibro-acoustic system data into an optimisation procedure was developed and applied to the case of a Fokker F70/100.

The primary field data were measured during flight at 36 locations, corresponding with the head positions in the aft cabin part. In an extensive ground test, the FRF matrix between all feasible second source locations and the target acoustic responses was determined.

In total 50 acoustical and 144 structural secondary source locations were identified.

Given the large complexity of mounting the exciting shakers at all locations, a reciprocal test procedure was adopted.

The optimisation was then performed for a maximum number of 45 actuators at three engine tones. A first optimisation was based on acoustic sources, a second one on structural sources. The cabin noise levels are optimised at 36 control sensors.

Different optimisation methods (forward build and spatial fit) were evaluated.

INTRODUCTION

Interior noise reduction in aircraft is a topic on which a considerable research effort is spent. Active noise control is one of the main topics addressed to this purpose. In the previous years, an extensive evaluation was made of the possibilities of pure acoustical control configurations using loudspeakers. For tonal noise (e.g. from blade-passage harmonics in propeller aircraft or rotor harmonics in turbofan aircraft), commercial systems have been developed and are being used industrially. Recent research has been directed to apply structural secondary sources in order to obtain a so-called "Structural Acoustics Control". This topic is also addressed in the Brite Aeronautics project "ASANCA 2".

In order to predict the performance of such systems and to optimise the actual configuration in terms of number and location of actuators and sensors, a methodology combining in-flight data with vibro-acoustic system data into an optimisation procedure was developed and applied to the case of tonal noise reduction in a Fokker F70/100 aircraft.

OPTIMISATION METHODOLOGY

The primary field, referred to as $\{p\}_n$ is a vector containing the in-flight acoustic response at n microphone positions. The secondary field $\{s\}_n$ is the sound field, at the same microphone positions, generated by the $\{q\}_m$ actuators. The resulting sound field, when the control is active, is called the residual field $\{e\}_n$. With $[H]_{n \times m}$, a matrix containing the transfer functions between the m actuator source strengths and n microphone responses, one may write

$$\{e\}_n = \{p\}_n - \{s\}_n = \{p\}_n - [H]_{n \times m} \{q\}_m^t \quad (1)$$

A "maximal" set of feasible secondary source locations is then defined, for which the $[H]_{n \times m}$ matrix is measured or predicted. An optimisation strategy is then adopted to search for an optimal subset of d sources. The vector containing the set of d corresponding source strengths is referred to as $\{q\}_d$. The optimisation can be calculated for a single spectral line or over a frequency band. Different procedures can be followed to this purpose [1,2,3,4]. In the present study, the "forward build" and the "spatial fit" methods were used. Although not necessarily leading to the global optimum, their performance is adequate and their application is straightforward.

Build Method The criterion used in the *build* method selects the additional d -th actuator which offers the best possible incremental noise reduction to a subset of $d-1$ actuators.

In step one of the optimisation procedure the over-determined equation $\{p\}_n = -\{H_j\}_n q_j$ is solved in a least square sense for all possible sources j . The solution of this equation q_j is the source strength that is needed to have a secondary field that is as close as possible to the (negative) primary field. This source strength q_j is used to calculate the secondary field $\{s\}_n = -\{H_j\}_n q_j$, the residual field $\{e\}_n = \{p\}_n + \{s\}_n$ and the norm $\|\{e\}_n\|$. The source actuator $s1$ for which $\|\{e\}_n\|$ is minimal is selected as the first actuator source.

In the next step an additional actuator is selected which gives the best possible reduction in combination with the first actuator $s1$. In order to determine this additional actuator source equation (2) is solved for all actuator sources j , except for the one already selected $s1$.

$$\{p\}_n = \left[\begin{array}{c} \{H_{s1}\}_n \\ \{H_j\}_n \end{array} \right]_{n \times 2} \left\{ \begin{array}{c} q_{s1} \\ q_j \end{array} \right\}_{2 \times 1} \quad (2)$$

The actuator $s2$ for which $\|\{e\}_n\|$ is minimal is selected as the second source. This procedure is repeated until the desired number of sources or the desired attenuation is reached:

$$\{p\}_n = \left[\begin{array}{c} \{H_{s1}\}_n \\ \{H_{s2}\}_n \\ \dots \\ \{H_{sd-1}\}_n \\ \{H_j\}_n \end{array} \right]_{n \times d} \left\{ \begin{array}{c} q_{s1} \\ q_{s2} \\ \dots \\ q_{sd-1} \\ q_j \end{array} \right\}_{d \times 1} \quad (3)$$

Spatial fit method In the *spatial fit* method, the procedure will look for the source with the best spatial correlation to the primary field rather than looking for the source with the best reduction. The idea is to have a better compromise between noise reduction and power consumption.

In the first step of the optimisation procedure the *spatial fit* (4) of all the columns $\{H_j\}_n$ of the transfer function matrix $[H]_{n \times m}$ to the primary field $\{p\}_n$ is calculated. The *spatial fit* of two vectors is the absolute value of their inner product divided by the norm of both vectors.

$$spf1_j = \frac{|\{H_j\}_n^H \{p\}_n|}{\|\{H_j\}_n\| \|\{p\}_n\|} \quad (4)$$

The value of the $spf1$ will always reside between 0 and 1. The larger this value, the better the vector $\{H_j\}_n$ corresponds to the primary field vector $\{p\}_n$. The actuator source j for which spf_j is maximal is selected as the first actuator source $s1$. The source strength, secondary field level, and residual field level are then calculated as discussed for the build method.

In the following steps the *spatial fit* (5) of all vectors $\{H_j\}_n$ to the residual field $\{e\}_n$ is calculated, where j is one of the not yet selected actuator sources.

$$spf1_j = \frac{|\{H_j\}_n^H \{e\}_n|}{\|\{H_j\}_n\| \|\{e\}_n\|} \quad (5)$$

The residual field $\{e\}_n$ is the sound field, when the already selected actuators are active.

In a variation of the method ("spf2"), the best actuator is selected based upon a different criterion.

$$spf2_j = \frac{|\{H_j\}_n^H \{p\}_n|}{\|\{p\}_n\|} \quad (6)$$

This criterion favours even more sources that lead to less power consumption. Suppose that you have two vectors $\{H_a\}_n$ and $\{H_b\}_n$ for which $spf1_a = spf1_b$, and for which the norm of $\{H_a\}_n$ is larger than the norm of $\{H_b\}_n$. This means that they have the same *spatial fit* for formula (5). But the *spatial fit* for formula (6) is not the same. In this case $spf2_a > spf2_b$, and as a consequence actuator a is selected. By adding an actuator with a good spatial correlation with the primary field, the resulting source strength q_a , and thus the power, will be smaller than for source b.

Finally, additional constraints limiting the maximum level of the actuators can be used.

TEST PROCEDURE

The primary field data were measured during flight at 574 locations in the aircraft cabin. This was done in view of an extensive vibro-acoustic mapping of the in-flight behaviour [5]. The tonal nature of the noise can be observed in figure 1 for a typical microphone position. The acoustic field at 2 engine tones is shown in figure 2.

For the present analysis, only 36 locations, corresponding with the head positions in the aft cabin part are used. The data were measured as referenced spectra (complex fields, coherent with engine tacho signal references). The objective of the ground tests then was to determine the FRF matrix between all feasible secondary source locations and the target acoustic responses.

In total 50 acoustical and 144 structural secondary source locations were identified.

Given the large complexity of mounting the exciting shakers at all locations, a reciprocal test procedure was adopted for the structural tests: the 144 possible second source locations were instrumented with accelerometers and loudspeaker excitation was applied at the target microphone locations. This conforms with the vibro-acoustical reciprocity [6,7,8].

Let p_j be the pressure, and \dot{q}_j , the volume acceleration at point j and \ddot{x}_i the acceleration and f_i the force at point i , then:

$$\frac{p_j}{f_i} \Big|_{\dot{q}_j=0} = \frac{\ddot{x}_i}{\dot{q}_j} \Big|_{f_i=0} \quad (7)$$

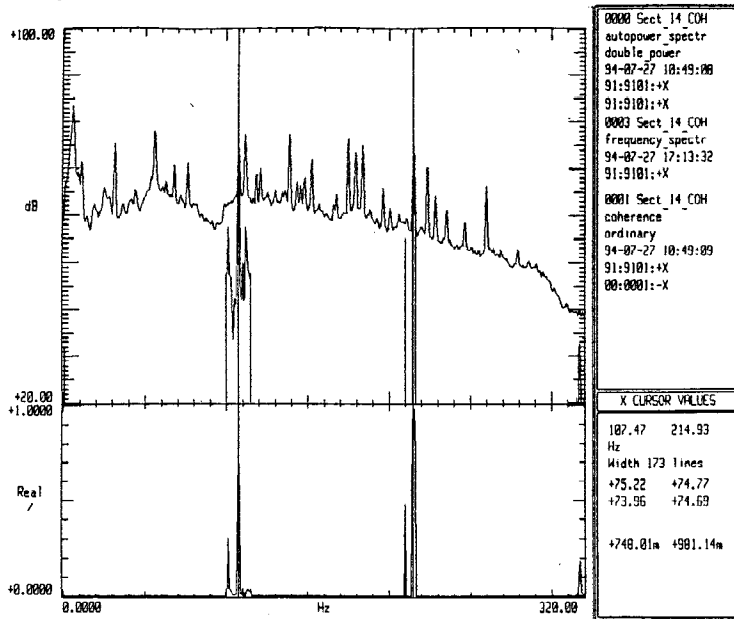


Figure 1: in-flight noise spectrum and right-engine coherence

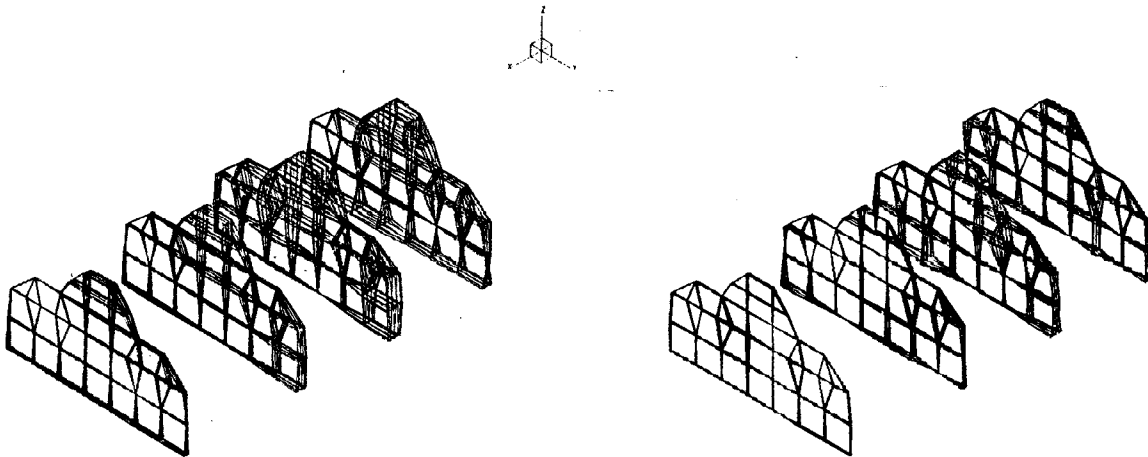


Figure 2: in-flight noise fields (1N1R, 2N1R)

This vibro-acoustic reciprocity was verified at a number of typical locations using hammer impact excitation (figure 3).

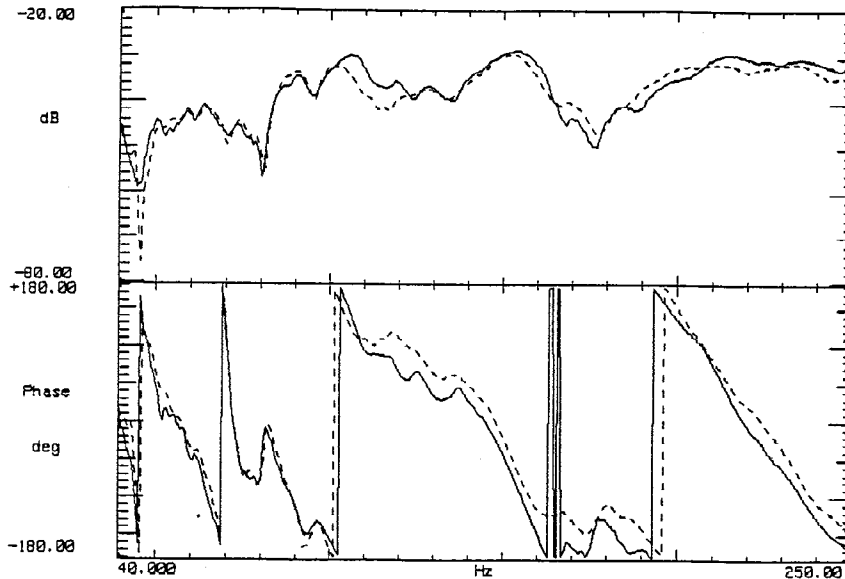


Figure 3: Reciprocity verification

OPTIMISATION STUDY: ACOUSTIC EXCITATION

For the case of acoustic excitation, the optimisation was performed using up to 42 anti-sound loudspeakers. The 3 methods (build - spatial fit - spatial fit 2) are compared with respect to overall noise reduction and total required source strength.

The optimisation is performed at one single frequency (1N1R). the results are presented in table 1 for up to 25 sources.

SOURCES	BUILD		SPATIAL FIT 1		SPATIAL FIT 2	
	RED[dB]	STRENGTH	RED[dB]	STRENGTH	RED[dB]	STRENGTH
1	2.85	0.12	2.85	0.12	2.85	0.12
2	4.25	0.13	4.25	0.13	4.25	0.13
3	5.43	0.22	4.83	0.14	4.70	0.14
4	6.57	0.27	5.29	0.15	5.20	0.13
5	8.08	0.34	5.55	0.16	6.18	0.16
6	9.38	0.56	6.05	0.19	6.57	0.16
7	9.71	0.58	6.65	0.17	7.39	0.19
8	10.23	0.57	7.85	0.20	8.05	0.21
9	10.62	0.48	8.25	0.25	8.96	0.21
10	11.09	0.47	9.11	0.27	9.06	0.22
11	11.44	0.43	9.70	0.27	9.25	0.21
12	11.97	0.46	10.28	0.30	9.36	0.22
13	12.31	0.46	10.95	0.29	10.03	0.25
14	12.63	0.47	11.42	0.29	11.61	0.28
15	13.03	0.46	12.03	0.30	12.07	0.28
16	13.28	0.44	12.34	0.31	12.26	0.28
17	13.68	0.49	12.42	0.31	12.42	0.29
18	14.15	0.47	12.71	0.32	12.48	0.30
19	14.46	0.59	12.90	0.32	12.66	0.32
20	14.75	0.61	13.07	0.32	12.85	0.32
21	14.94	0.58	13.20	0.31	12.97	0.32
22	15.20	0.66	13.42	0.34	13.25	0.36
23	15.42	0.89	13.72	0.63	13.33	0.36
24	15.67	1.03	13.92	0.77	13.46	0.36
25	15.88	1.10	14.38	0.70	13.52	0.34

Table 1: acoustic excitation comparison

The build procedure proves superior in noise reduction performance, whereas the spatial fit 1 method does not yield the expected reduction in total source power. For a given value of noise reduction, the spatial fit 2 method proves slightly better with respect to required power, but at the cost of an increased number of sources. However, the source levels are much more uniform, whereas in the build method larger differences occur which may cause constraints for practical application. A clear "saturation effect" in terms of incremental noise reduction for an increased number of actuators is encountered.

OPTIMISATION STUDY : STRUCTURAL EXCITATION

The optimisation was then performed for a maximum number of 30 structural actuators. For this study, results at three engine tones (0.5NR1, 1NR1 and 2NR1) were used. The cabin noise levels are again optimised at 36 control sensors.

The results are given in table 2 for up to 25 exciters using the "build" method. For each step of the optimisation procedure the selected actuator source is printed together with the obtained reduction and necessary power.

In a second step, the optimisation was performed for the three engine tones together. The results for this optimisation are given in table 3. The "spatial fit results" again correspond well with the "build" ones, with a slightly smaller reduction, but a more efficient actuation in terms of source strength and more uniform source level distribution.

SOURCES	0.5NR1		1NR1		2NR1	
	RED [dB]	STRENGTH	RED [dB]	STRENGTH	RED [dB]	STRENGTH
1	0.51	4.72	4.65	16.61	1.46	23.99
2	0.94	5.79	5.94	20.99	2.14	19.33
3	1.79	4.88	7.78	45.84	2.55	18.11
4	2.35	5.01	9.10	47.61	2.97	18.13
5	2.65	6.36	10.11	47.20	3.41	16.96
6	2.93	7.18	11.43	88.02	3.76	17.99
7	3.15	7.17	12.26	122.85	4.22	21.59
8	3.41	7.59	12.90	112.91	4.90	22.99
9	3.71	8.73	14.12	130.79	5.27	24.14
10	4.25	11.06	15.01	136.30	6.05	27.14
11	4.52	12.69	15.63	127.74	6.57	30.42
12	4.92	13.95	16.28	121.58	6.94	32.77
13	5.21	15.25	16.87	110.40	7.50	34.32
14	5.95	16.29	17.73	113.28	7.86	37.11
15	6.52	17.94	18.34	120.94	8.41	35.57
16	6.97	20.40	18.97	114.25	8.99	44.16
17	7.48	21.16	20.07	118.49	9.53	65.36
18	8.08	22.27	21.67	130.00	10.37	103.95
19	8.74	24.63	22.29	133.63	11.06	114.37
20	9.52	27.08	22.90	134.90	12.19	105.03
21	10.30	28.42	23.55	136.13	14.14	142.57
22	11.38	27.96	24.51	137.18	16.05	167.21
23	12.19	28.60	25.11	147.66	17.11	166.93
24	12.77	28.84	25.73	152.62	18.19	187.32
25	13.31	28.35	26.77	167.01	12.33	188.54

Table 2: structural excitation results

	<i>0.5NRI + 1NRI + 2NRI</i>	
<i>SOURCES</i>	<i>RED [dB]</i>	<i>STRENGTH</i>
1	3.86	6.12
2	4.87	8.04
3	6.23	16.91
4	7.26	21.51
5	8.00	21.45
6	8.65	31.46
7	9.33	31.50
8	9.94	36.35
9	10.46	42.31
10	11.02	43.19
11	11.46	42.87
12	11.96	49.58
13	12.96	49.50
14	13.73	49.44
15	14.41	56.19
16	14.93	58.78
17	15.47	59.36
18	16.10	60.14
19	17.16	61.46
20	17.76	65.34

Table 3: structural excitation - combined results

COMPARISON OF STRUCTURAL AND ACOUSTICAL EXCITATION

Finally, the performance of structural versus acoustic excitation was compared for the case of single-frequency excitation (1N1R). The results are shown in figure 4.

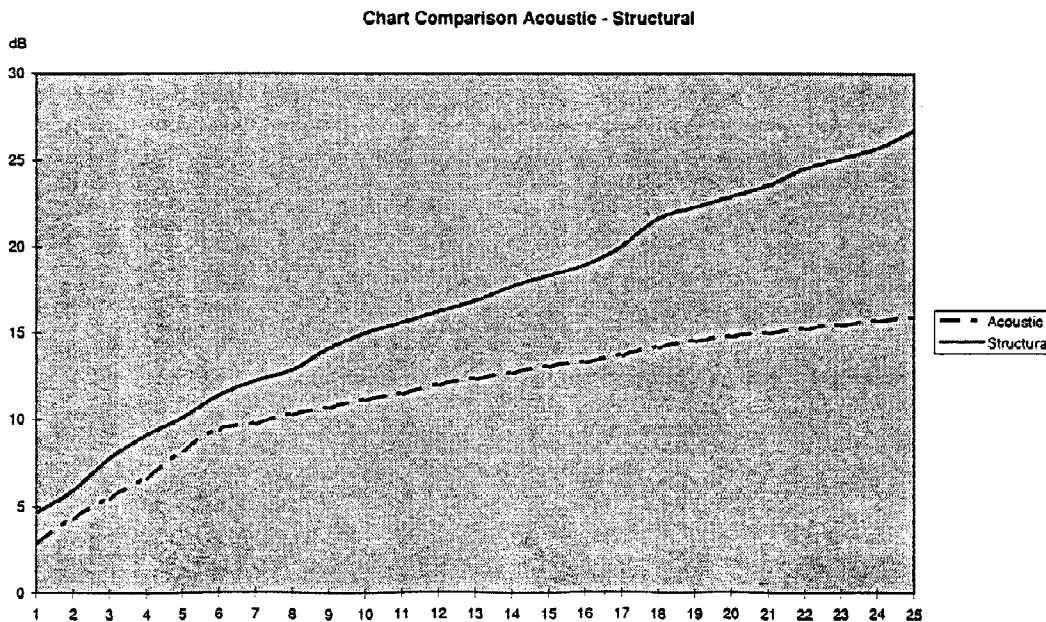


Figure 4: structural versus acoustic excitation - results

An important conclusion is that the incremental noise reduction for an additional structural source is larger than in the case of acoustic excitation and that consequently, for the compared frequency, structural actuation is much more effective than acoustic excitation. This conclusion cannot be generalised. Similar studies in other aircraft [9] do not confirm the generality of this conclusion. Probably the strong structure-borne nature of the noise problem in the rear cabin part of the Fokker 100 lies at the origin of this finding.

ACKNOWLEDGEMENT

The presented research was conducted in the framework of Brite project AER2-0062, "ASANCA-2". The support of the EC is gratefully acknowledged.

REFERENCES

- [1] RUCKMAN C.E., FULLER C.R., *Optimizing actuator locations in feedforward active control systems using subset selection*, Proc. 2nd Conference on Recent Advances in Active Control of Sound and Vibration, Blackburg (VA), April 28-30, 1993, pp. S122-S133.
- [2] WYCKAERT K., VAN DER AUWERAER H., HERMANS L., *An approach for the simulation of active control sensor and actuator configurations for rolling noise in automotive vehicles*, Proc. Active '95, Newport Beach (CA), July 6-8, 1995, pp. 747-754.
- [3] WYCKAERT K., DEHANDSCHUTTER W., BANFO G.L., *Active vibration control of rolling noise in a passenger car: Performance evaluation of actuator and feedback sensor configuration*, Proc. Active '95, Newport Beach (CA), July 6-8, 1995, pp. 755-766.
- [4] TSAHALIS D.T., KATSIKAS S.K., MANOLAS D.A., *A genetic algorithm for optimal positioning of actuators in active noise control results from the ASANCA project*, Proc. Inter-Noise '93, Leuven (B), August 24-26, 1993, pp. 83-88.
- [5] VAN DER AUWERAER H., OTTE D., BRUGHMANS M., WATERMAN E., REIJNEN J., *Primary Sound field characterisation of the Fokker 100 using experimental and numerical vibro-acoustical models*, Proc. Noise-Con '96, Seattle (WA), Sept. 29 - Oct. 2, 1996, pp. 187-192.
- [6] VAN DER LINDEN P.J.G., FUN J.K., *Using mechanical-acoustical reciprocity for diagnosis of structure-borne sound in vehicles*, Proc. 1993 Noise and Vibration Conference, SAE paper 931340, Traverse City, May 10-13, 1993, pp. 625-630.
- [7] FAHY F.J., *The reciprocity principle and applications in vibro-acoustics*, Proc. of the 2nd International Congress on Recent Developments in Air- and Structure-Borne Sound and Vibration, Auburn, March 4-6, 1992, pp. 611-618.
- [8] WYCKAERT K., AUGUSZTINOVICZ F., *Vibro-acoustic modal analysis: Reciprocity, model symmetry and model validity*, International Seminar on Modal Analysis, Leuven (B), 1995.
- [9] VAN DER AUWERAER H., IADEVAIA M., EMBORG U., GUSTAVSSON M., *Derivation of experimental vibro-acoustical models for ANC configuration design*, Proc. 3rd AIAA/CEAS Acoustics conference, Atlanta (GA), May 12-14, 1997, paper nr. AIAA-97-1618.